Adsorption and Hydrogenation of Carbon Monoxide on Polycrystalline Rhodium at High Gas Pressures

Christopher T. Williams,[†] Carol A. Black,[†] Michael J. Weaver,*[,‡] and Christos G. Takoudis*[,†,§]

School of Chemical Engineering and Department of Chemistry, Purdue University, West Lafayette, Indiana 47907

Received: October 31, 1996; In Final Form: February 6, 1997[⊗]

Surface-enhanced Raman spectroscopy (SERS) in conjunction with mass spectroscopy (MS) has been utilized to investigate the adsorption and hydrogenation of carbon monoxide on polycrystalline rhodium surfaces. The SERS-active Rh substrates were prepared by electrodeposition of ultrathin films on electrochemically roughened gold and display remarkably robust SERS activity over a wide range of temperatures (up to 400 °C) and pressures (here up to 1 atm). The SER spectra reveal that CO adsorbed primarily on atop sites ($\nu_{Rh-C} = 470$ cm^{-1}) and desorbed by about 250−300 °C under all gas-phase conditions examined. Partial dissociation of the CO adlayer, however, was obtained at temperatures as low as 100 °C, most likely facilitated by the large number of steps and kinks present on these roughened surfaces. This was evidenced by a partial removal of CO at temperatures (ca 100 °C) well below those expected for thermal desorption (200−250 °C) and supported by the observed formation of surface carbonate (665 cm^{-1}) under these conditions. The CO dissociation, however, is hampered at lower temperatures (<200 °C) when gas-phase H_2 and/or CO are present, most likely due to blocking of site ensembles necessary for decomposition to proceed. Interestingly, heating a CO adlayer in pure H_2 resulted in the formation of an adsorbed oxygen species ($\nu_{Rh-O} = 295$ cm^{-1}) at temperatures above 250 °C. The CO hydrogenation reaction was examined over a wide range of gas-phase conditions (H_2:CO = 99:1 to 4:1 at 1 atm), with methane being the only hydrocarbon product detectable with MS. In addition to the presence of adsorbed CO observed up to 250 °C under all H_2/CO reaction ratios, the adsorbed oxygen species noted above was detected at higher temperatures (>250 °C) when a low percentage of CO (≤1%) in the feed reactant stream was used. The influence of the adsorbed species on the overall methanation rates is discussed in light of these findings. Utilizing the seconds time-scale resolution of SERS, the exchange between gas-phase and adsorbed CO was also studied. The results of such transient ^{13}CO/^{12}CO exchange experiments reveal that this desorption pathway is weakly activated (≈1 kcal mol^{-1}), first order with respect to CO coverage, yet independent of CO partial pressure in the regime studied (8−760 Torr). This contrasts the first-order pressure dependence for much lower CO partial pressures (≤10^{-5} Torr) reported earlier in the literature. A rate law and mechanism are proposed which account for these differences and rationalize the observed behavior.

Introduction

The interaction of carbon monoxide with rhodium surfaces has been well scrutinized over the past 20 years. Additionally, CO hydrogenation is a surface process that has received much attention. As well as its technological significance regarding the formation of hydrocarbons and/or oxygenates, the chemical richness of the CO + H_2 reaction makes it interesting from a fundamental standpoint. A major focus has been placed on the factors that determine selectivity toward any one of the numerous possible reaction products. On polycrystalline,[1,2] single-crystal,[2] and supported Rh surfaces,[3−8] methane is predominantly formed along with much smaller amounts of other hydrocarbons. However, oxygenate formation has been observed over some types of supported Rh[9−11] and on rhodium oxide surfaces.[2,12] These investigations reveal that selectivity is highly dependent on a number of experimental parameters, including support material, temperature, pressure, and the reactant ratio utilized. Numerous surface reaction intermediates have been reported, including carbon,[1,4,6,13] subsurface oxygen,[1] ethylidene,[14] carbonyl hydride,[8,15,16] CH_x,[5] methoxy,[10,11,17] ethoxy,[10,11,17] formate,[4] and carbonate,[4,9] although in many instances these species are present only on the catalyst support.[4,10,11,17] As they are central to understanding the mechanism of this reaction, the rate and extent of CO dissociation on rhodium surfaces have also been investigated.[1,13,18−23] It is generally accepted that the probability for CO decomposition is greatest on stepped and kinked surfaces.[1,13,20−23]

However, while much has been discovered about the interaction of CO with H_2 on single-crystal and supported Rh, there are very few studies involving polycrystalline surfaces.[1,2] More importantly, neither of these involves the monitoring of reaction intermediates *in situ* at high gas pressures of more direct technological significance. While many of the intermediates mentioned above for supported catalysts may be of mechanistic significance, it is still important to determine which species would form *independently* if there were no influence from the support material. We have demonstrated in previous papers[24−32] how surface-enhanced Raman spectroscopy (SERS) can be used as an interfacial probe of heterogeneous catalytic reaction systems. One process that has been of particular interest to us is NO reduction on Rh,[24,26,27,29−31] Pt,[32] and Pd.[32] The surfaces utilized for these studies were electrochemically deposited transition-metal thin films on roughened SERS-active gold substrates. These surfaces exhibit stable as well as intense SERS activity, even at elevated temperatures, and largely mimic the

[†] School of Chemical Engineering.
[‡] Department of Chemistry.
[§] Presently with the Department of Chemical Engineering, University of Illinois at Chicago.
[⊗] Abstract published in *Advance ACS Abstracts,* March 15, 1997.

S1089-5647(96)03429-3 CCC: $14.00

adsorptive and catalytic behavior of their transition-metal analogues. One advantage of this approach is the ability to monitor adsorbed oxygen and other species, X, from their characteristic surface−X vibrations, since SERS is sensitive to modes in this low-frequency (200−1000 cm^{-1}) region. The advent of charge coupled device (CCD) technology along with the intrinsically intense SERS signals also allows the acquisition of spectra on a seconds time scale, thereby enabling us to probe the temporal evolution of surface species by perturbing the system parameters (e.g., temperature, reactant ratio) and monitoring the transient spectroscopic response. Kinetic measurements obtained simultaneously during real-time SERS measurements by means of mass spectrometry (MS) allow for direct correlations to be made between overall rates of reaction and surface speciation.[29,31,32]

In this paper we report the results of a detailed SERS study involving the adsorption, desorption, and dissociation of carbon monoxide on a polycrystalline rhodium surface in the absence and presence of gas-phase CO. Furthermore, we present complementary SERS and MS results regarding the reaction of CO with H_2 at several reaction conditions with a view toward determining which surface species may have a direct influence upon the reaction mechanism.

Experimental Section

The SERS-active rhodium films were prepared utilizing 6 mm diameter disks cut out of 0.1 mm thick gold foil (99.95% pure, Johnson Matthey), and polished using 0.3 μm alumina powder. They were then placed into an electrode holder that exposed ca. 7 mm^2 of the surface and subjected to 25 oxidation−reduction cycles from −0.3 to 1.2 V vs SCE at 0.5 V s^{-1} in 0.1 M KCl to produce the surface roughness necessary for Raman enhancement.[33] The surface was rinsed thoroughly with deionized water and subsequently transferred to another cell for electrochemical deposition of the Rh overlayers. The procedure for Rh deposition utilized a 0.3 mM solution of $RhCl_3$ in 0.1 M $HClO_4$ at 0.1 V vs SCE. The cathodic charge was monitored and controlled in order to limit the deposition to the desired film thickness, usually between 2 and 5 equivalent monolayers.[34,35] This choice of rhodium film conditions has been found to optimize the SER spectral response.[28,34,35]

The reactor utilized for the SERS experiments consists of a 100 cm^3 volume six-way cross, equipped with a turbomolecular pump (Balzers TPH 060) yielding a base pressure of 2×10^{-6} Torr. A combination of needle, gate and butterfly valves allows operation of the reactor at pressures ranging from 10^{-3} to 760 Torr. The pressure over the entire range is measured using a combination of Pirani and cold-cathode gauges, controlled by a Balzers TPG 252 pressure controller. One of the reactor arms contains an optical viewport, over which the specimen is mounted on a stainless steel cylindrical sample holder which can be heated to 500 °C. Inside the sample holder, a solid piece of stainless steel is surrounded by a coil of thin Nichrome wire to provide resistive heating. Through the center of this heater is a K-type thermocouple which leads to a programmable temperature controller (Omega CN2041). Laser excitation is provided by a Kr^+ laser at 647.1 nm (Spectra Physics), and scattered light is collected by a three-stage spectrometer (SPEX Triplemate). The spectrometer is equipped with a liquid nitrogen-cooled Photometrics CCD, allowing acquisition of real-time spectral sequences typically even on a seconds time scale with a good signal-to-noise ratio. The reactants are introduced into the reactor through a manifold that allows mixing of up to four inlet gases and flow rates are measured with a bubble flow meter. Gases were obtained from Airco (>99.9% purity) and were used without further purification. The isotopes utilized in this study were obtained from Cambridge Isotope Laboratory (99% pure ^{13}CO, 98% pure $^{18}O_2$) and Matheson (99% pure D_2) and were used without further purification.

As the surface area of the substrate utilized for SERS was too small (0.07 cm^2) to yield reliable kinetic data, a higher surface area version was prepared. This consisted of a 5 m long, 0.05 mm diameter gold wire (99.998% pure, Johnson Matthey) that was subjected to the same oxidation−reduction cycling and Rh deposition described above and provided a catalyst with ca. 7 cm^2 surface area. The reactions were carried out in a small-volume (4 cm^3) stainless steel reactor (Spectra Physics) that could be evacuated to 10^{-6} Torr via a turbopump. Gas-phase composition was measured by leaking the gas outlet into a Lybold Inficon IPC-50 quadrupole mass spectrometer.

Results and Discussion

The electrochemically deposited Rh thin films were pretreated by heating to ca. 150 °C in 100 cm^3 min^{-1} of H_2 for about 5 min. This procedure resulted in a clean SERS background in the 200−1000 cm^{-1} range but retained features in the 1300−1600 cm^{-1} region due to surface carbonaceous residues. Complete removal of these bands required prior high-temperature oxidation, which resulted in severe disruption of the film and substantial loss of SERS activity following reduction; this was therefore not used as part of the pretreatment procedure in the following experiments.

Before proceeding, it is worthwhile to review our previous efforts with regard to adsorption of CO on rhodium surfaces. In earlier SERS studies[24,26,27] it was found that CO adsorbed primarily in a terminal configuration on thin Rh films, as discerned by the observed frequencies of the Rh−CO stretching (ν_{Rh-C} = 465 cm^{-1}) and C−O stretching (ν_{C-O} = 2040 cm^{-1}) vibrations. Similar observations were made more recently during a combined SERS and MS investigation of the NO−CO reaction on rhodium.[29] However, several aspects of CO adsorption on these rough polycrystalline Rh surfaces have not yet been examined, including the desorption behavior and extent of dissociation. With regard to the former, the time resolution afforded by SERS (*vide supra*) enables the monitoring of CO desorption in both the presence and absence of gas-phase CO. In the case of the latter, the sensitivity of SERS to low-frequency (<800 cm^{-1}) Rh−adsorbate vibrations is useful for detecting dissociation products such as adsorbed oxygen.

Adsorption and Dissociation of CO. The desorptive and dissociative behavior of adsorbed CO was first investigated. A reduced Rh surface was exposed to 1 atm of CO at 25 °C, followed by evacuation of the reactor to ca. 10^{-5} Torr. Nitrogen was then introduced at a flow rate of 100 cm^3 min^{-1}, with typical low-frequency SER spectra as presented in Figure 1A. Unless otherwise noted, a spectral acquisition time of 10 s was employed for all SER spectra reported. The 25 °C spectrum (bottom) reveals the presence of the expected 470 cm^{-1} band assigned to the ν_{Rh-C} stretch of terminally adsorbed CO (*vide supra*). Furthermore, examination of the higher frequency region (1800−2300 cm^{-1}) revealed the corresponding ν_{C-O} stretch at 2040 cm^{-1} (not shown). The sample was subsequently heated at a rate of ca. 0.5 K s^{-1} in a stepwise periodic fashion, remaining at each temperature until the spectra became time independent (ca. 1−2 min). This same heating protocol was utilized for all further experiments unless otherwise noted. The intensity of the ν_{Rh-C} band was seen to decrease as the temperature was raised, with complete removal occurring by 300 °C. As expected, a similar temperature-dependent behavior was observed for the corresponding 2040 cm^{-1} ν_{C-O} stretch

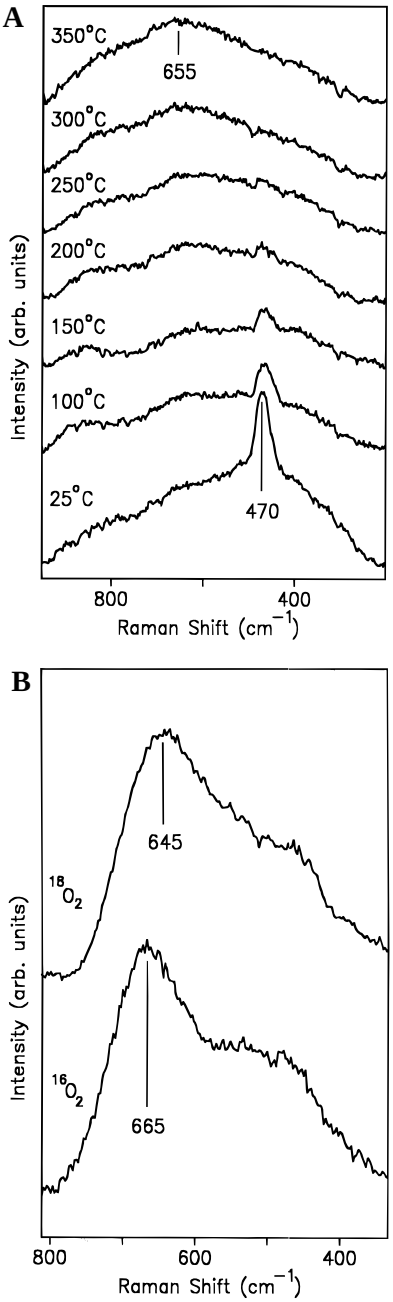

Figure 1. (A) Temperature-dependent SER spectra of a CO-saturated Rh surface exposed to 100 cm^3 min^{-1} of pure N_2 at 1 atm. The temperature was raised in a stepwise manner, starting at 25 °C, to the values indicated. Integration time for each spectrum was 10 s. (B) SER spectra of a Rh surface exposed to 100 cm^3 min^{-1} of 80% O_2/20% CO at 350 °C and 1 atm utilizing $^{16}O_2$ (bottom spectrum) and $^{18}O_2$ (top spectrum). Integration time for each spectrum was 10 s.

(not shown). Additionally, a broad feature at 655 cm^{-1} became evident by 100 °C and increased slightly with further heating. In our recent SERS investigation of the CO−NO reaction on Pt and Pd, an apparently similar band was observed under reaction conditions and was tentatively assigned to a surface carbonate species formed by the reaction between surface carbonaceous impurities and oxygen.[32] Interestingly, we have also noted the formation of an apparently similar 655 cm^{-1} feature during reaction between CO and excess O_2 on Rh at high pressures and elevated temperatures (Figure 1B). The substitution of $^{18}O_2$ under those conditions resulted in a ca 20 cm^{-1} downshift (Figure 1B), confirming the presence of oxygen in the species responsible for the vibration. The frequency of this 655 cm^{-1} band is similar to SERS features observed during

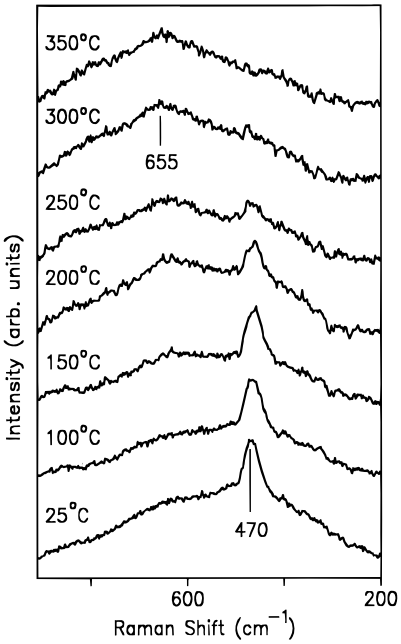

Figure 2. Temperature-dependent SER spectra of a Rh surface exposed to 100 cm^3 min^{-1} of pure CO at 1 atm. The temperature was raised in a stepwise manner, starting at 25 °C, to the values indicated. Integration time for each spectrum was 10 s.

adsorption of CO_3^{2-} on silver electrodes[36a,b] and is consistent with the δ_a asymmetric normal mode of adsorbed carbonate.[36c] Furthermore, we would expect at least a 10−15 cm^{-1} downshift in the frequency of this vibration with ^{18}O substitution due to the participation of all three oxygen atoms in the vibration; this is consistent with the observed behavior. Thus, the 655 cm^{-1} feature observed here is tentatively assigned to surface carbonate.

Heating a CO adlayer in the presence of gas-phase CO yielded somewhat different results, as shown in Figure 2. The procedure utilized was identical to that described above for Figure 1A, except that the sample was heated in 100 cm^3 min^{-1} of CO at 1 atm rather than N_2. In contrast to the behavior observed during CO desorption in the absence of gas-phase CO, the intensity of the 470 cm^{-1} ν_{Rh-C} band remained unchanged as the temperature was raised to 150 °C. However, further heating resulted in an intensity decrease starting at 200 °C, with eventual removal of adsorbed CO by 350 °C. The 655 cm^{-1} feature became evident above 150 °C (Figure 2), and its intensity increased markedly as the temperature was elevated further.

The significant apparent decrease in the surface concentration of CO by 100 °C upon heating in N_2 (Figure 1A) differs from thermal desorption studies of CO from polycrystalline rhodium surfaces into vacuum, which report desorption temperatures in excess of 150 °C.[1,18] Thus, another explanation for this marked intensity decrease of the 470 cm^{-1} ν_{Rh-C} feature is suggested. A plausible cause for this finding is that a portion of the CO adlayer has dissociated by 100−150 °C. Indeed, several investigations have shown that CO dissociates on rhodium at elevated temperatures,[1,13,20−23] albeit to a small extent. For instance, CO dissociation has been reported in temperature-programmed desorption (TPD) studies by Somorjai and co-workers on polycrystalline[1] and highly stepped single-crystal[20] Rh surfaces. A high-temperature (ca. 700 °C) CO desorption peak was attributed to the recombination of carbon and oxygen produced from dissociation at lower temperatures.[1,20] The apparent observation of CO dissociation on the roughened substrates examined here is consistent with the previous findings

that indicate that this process is enhanced on stepped and kinked surfaces.[1,13,20−23]

The apparent formation of surface carbonate under these conditions (*vide supra*) may also be a consequence of CO dissociation. The two formation pathways involve the reaction of adsorbed CO and/or surface carbon with adsorbed oxygen formed by CO dissociation, as indicated in eqs 2a and 2b, respectively (S denotes a free site):

$$CO_{(ads)} + S \rightleftharpoons C_{(ads)} + O_{(ads)} \quad (1)$$

$$CO_{(ads)} + 2O_{(ads)} \rightleftharpoons CO_{3(ads)} + 2S \quad (2a)$$

$$C_{(ads)} + 3O_{(ads)} \rightleftharpoons CO_{3(ads)} + 3S \quad (2b)$$

The carbonate suggested by the 655 cm^{-1} band in the present study is stable up to at least 400 °C, possibly suggesting that the carbon and oxygen exist in this form before eventually breaking apart and desorbing as CO at higher temperatures. However, another explanation of the formation of carbonate may be that CO is reacting with oxygen impurities that may be present in the system. Thus, the presence of this moiety is not alone sufficient to imply that CO dissociation has occurred.

Interestingly, the presence of gas-phase CO appears to hamper dissociation at lower temperatures. While the marked intensity decrease of the 470 cm^{-1} ν_{Rh-C} band by 100 °C during heating in pure N_2 indicated that some CO was dissociating (Figure 1A), the intensity of this feature remained essentially unchanged until 200 °C in the presence of gas-phase CO (Figure 2). The most likely explanation for this latter result is that CO blocks sites necessary for decomposition at lower temperatures. Such a site-blocking mechanism is consistent with the experimental results of Sachtler and Ichikawa, who showed that blocking a small fraction of Rh sites with Zn ($\theta_{Zn} \approx 0.2$) resulted in a marked decrease in CO dissociation activity.[37] Furthermore, de Koster et al. showed via *ab-initio* quantum chemical calculations that CO dissociation requires an ensemble of 5−7 free surface atoms.[38]

Interaction of Adsorbed CO with H_2. Prior to probing the state of a Rh surface during exposure to various reactive mixtures, the behavior of adsorbed CO was examined in the presence of pure hydrogen. This was prompted by the desire to isolate any effects that hydrogen may exert on CO desorption and dissociation. After exposing a reduced Rh surface to 1 atm of CO, the reactor was evacuated and the sample was exposed to 100 cm^3 min^{-1} of H_2. This was followed by heating the sample in a stepwise fashion, with typical SER spectra shown in Figure 3. At 25 °C, the 470 cm^{-1} band associated with terminal carbon monoxide is clearly seen. This band remained unaltered until about 150−200 °C, where its intensity began to decrease and a weak feature becomes discernible at 390 cm^{-1}. A similar band has been observed previously during high-resolution electron energy loss spectroscopic (HREELS) studies of CO−H_2 interactions with Rh(100) and was assigned to the ν_{Rh-C} stretch of CO adsorbed at 2-fold bridging sites.[39,40] In the same investigation, H_2 saturation of dilute CO adlayers resulted in conversion from a terminal to bridging configuration, qualitatively similar to the behavior observed here. This effect apparently results from strong repulsive forces, coupled with segregation of CO and atomic hydrogen within the adlayer. Further heating resulted in complete removal of adsorbed CO by 300 °C, accompanied by the appearance of a lower frequency peak at 295 cm^{-1} (Figure 3), which survived up to at least 350 °C. The assignment of this feature will now be considered.

In contrast with the significant dissociation observed during heating in N_2 (Figure 1A), the concentration of terminal CO

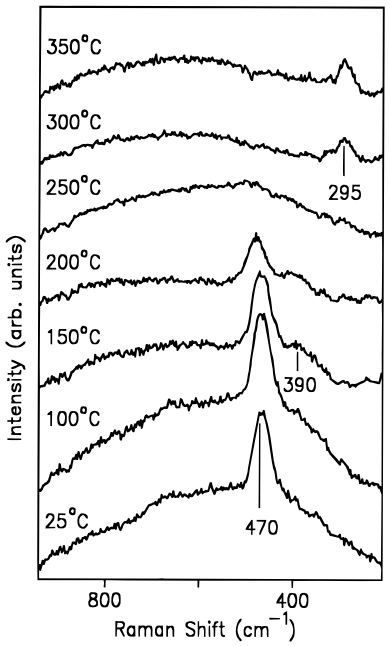

Figure 3. Temperature-dependent SER spectra of a CO-saturated Rh surface exposed to 100 cm^3 min^{-1} of pure H_2 at 1 atm. The temperature was raised in a stepwise manner, starting at 25 °C, to the values indicated. Integration time for each spectrum was 10 s.

remained unchanged until higher temperatures (ca. 150−200 °C). It therefore appears that the presence of H_2 can also inhibit CO decomposition at lower temperatures, most likely by a site-blocking effect similar to that mentioned above. Notwithstanding this, however, there does appear to be some CO dissociation at elevated temperatures in the presence of H_2. As heating a Rh surface in pure H_2 resulted in no discernible SERS features at elevated temperatures (*vide supra*), the emergence of the 295 cm^{-1} band at ca. 300 °C indicates that the interaction of adsorbed hydrogen and CO has resulted in the production of a new species. The low vibrational frequency of this band indicates that it is arising from a Rh−adsorbate stretch or bend. Experiments similar to that shown in Figure 3 were performed involving ^{13}CO and D_2 in order to determine the origin of this vibration. By employing a simple harmonic oscillator approximation[41] for Rh−adsorbate vibrations, a downward shift of at least 10 cm^{-1} is predicted upon $^{13}C/^{12}C$ or D/H isotope substitution for numerous carbon or hydrogen-containing species (e.g., CH_x, OH). As no frequency downshift for the 295 cm^{-1} peak was detected when either ^{13}CO or D_2 was employed, however, it is more likely that this vibration is arising instead from a Rh−O stretch of some type of adsorbed oxygen.

In order to determine the likelihood that such an oxygen species could be stable at high temperatures in the presence of H_2, that is, provide a plausible origin of the present 295 cm^{-1} feature, the following experiment was performed. A reduced Rh sample was first oxidized in 100 cm^3 min^{-1} O_2 at 200 °C for 5 min and cooled to 25 °C. This produced a surface covered by Rh_2O_3, as evidenced by the Rh−O stretch at 540 cm^{-1}, and another distinct form of adsorbed oxygen ($\nu_{Rh-O} = 290$ cm^{-1}), consistent with previously recorded SER spectra of oxidized Rh films.[28] Following evacuation of the reactor, the sample was exposed to 100 cm^3 min^{-1} of H_2 at 1 atm and heated in a stepwise fashion, with typical results shown in Figure 4. Both features were attenuated as the temperature was raised, with Rh_2O_3 and the other oxygen species being removed by 150 and 250 °C, respectively. Interestingly, however, a new feature at 290 cm^{-1} appeared at 300 °C and increased in intensity as the temperature was raised to 350 °C. Substituting $^{18}O_2$ for $^{16}O_2$

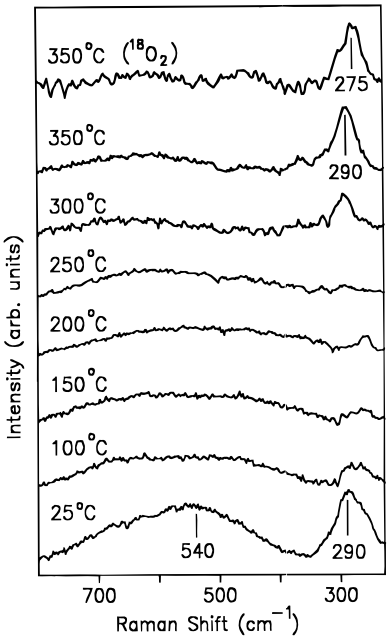

Figure 4. Temperature-dependent SER spectra of a previously oxidized Rh surface exposed to 100 cm^3 min^{-1} of pure H_2 at 1 atm. The temperature was raised in a stepwise manner, starting at 25 °C, to the values indicated. Integration time for each spectrum was 10 s. The top spectrum was obtained at 350 °C for the same experimental conditions, but utilizing an $^{18}O_2$-oxidized surface.

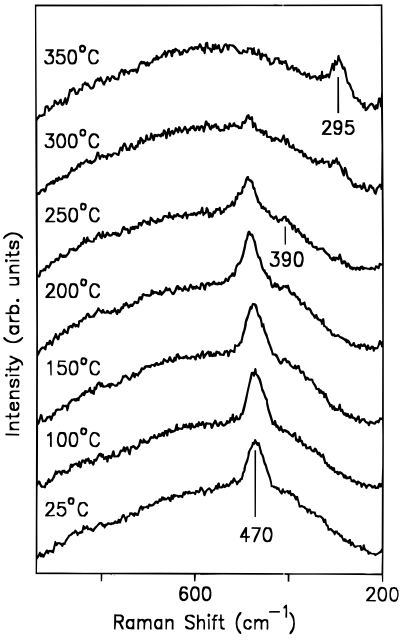

Figure 5. Temperature-dependent SER spectra of a Rh surface exposed to 100 cm^3 min^{-1} of a 99% H_2/1% CO mixture at 1 atm. The temperature was raised in a stepwise manner, starting at 25 °C, to the values indicated. Integration time for each spectrum was 10 s.

in the above experiment (Figure 4, top spectrum) resulted in a ca. 15 cm^{-1} frequency downshift in this 290 cm^{-1} band, confirming that oxygen is present in the species responsible for this vibration, probably as the lead-in (i.e., surface-bound) atom. As Rh_2O_3 extends at least 3 monolayers into the rhodium thin film,[28] a significant amount of subsurface oxygen must exist after the reduction of this species at 150 °C. In addition to numerous reports of subsurface oxygen on rhodium surfaces,[1,43,44] XPS measurements of oxidized Rh thin films have indicated the presence of such a species at temperatures higher than 200 °C.[28] Therefore, the high-temperature 290 cm^{-1} feature observed in Figure 4 can reasonably be attributed to adsorbed oxygen, which results from the diffusion of lattice oxygen closer to the surface. Most notable is the stability of this moiety at elevated temperatures in the presence of H_2 in the present case.

On the basis of these observations and the evidence garnered from the ^{13}CO and D_2 isotopic labeling experiments (*vide supra*), we assign the 295 cm^{-1} feature observed during heating a CO-saturated Rh surface in H_2 (Figure 3) to adsorbed atomic oxygen formed following CO dissociation. This oxygen may reside just below the first layer of Rh, which would explain its stability in the presence of H_2. Based on this interpretation, the differences between heating a CO-covered Rh surface in N_2 (Figure 1A) and H_2 (Figure 3) can be understood. In the former case, oxygen and carbon formed from CO dissociation at 100 °C may remain on the surface (possibly in the form of a carbonate species) or react to form CO_2. However, in the latter case the dissociation occurs at higher temperatures (ca. 200−250 °C), with any carbon reacting with hydrogen and leaving oxygen on the surface. This latter result appears to be consistent with the results of Somorjai and co-workers,[1,2] who observed the formation of subsurface oxygen and carbon during the reaction of CO and H_2 on polycrystalline Rh.

Steady-State Reaction of CO + H_2. In order to establish whether any of the above species and their related processes may be significant in influencing pathways for the CO−H_2 reaction, SERS measurements were obtained during stepwise surface heating in the presence of various mixtures of CO and H_2. The first ratio examined was a 99:1 H_2:CO mixture, and the behavior was found to be very similar to the case of heating a CO adlayer in pure H_2 (Figure 3). A rhodium surface was exposed to 100 cm^3 min^{-1} of 99% H_2/1% CO at 1 atm total pressure and heated in a stepwise fashion. Typical SER spectra obtained during such a procedure are presented in Figure 5, with the 470 cm^{-1} band associated with terminal CO observed at 25 °C (bottom spectrum). The concentration of this species remains relatively unchanged until ca. 200 °C, where a fraction of the CO adlayer switched to a bridging geometry, as evidenced by a slight appearance of the 390 cm^{-1} feature. Further heating resulted in the removal of the CO bands by 350 °C, which was about 100 °C higher than the removal temperature of CO in the presence of pure H_2 (Figure 3). Additionally, the 295 cm^{-1} oxygen feature appeared at 300 °C and grew notably stronger upon heating to 350 °C.

Increasing the amount of gas-phase CO in the reactant flow results in the disappearance of the 295 cm^{-1} oxygen feature. This effect is best illustrated via a transient experiment involving switching from one reactant ratio to another. A Rh surface was initially heated to 300 °C in 1000 cm^3 min^{-1} of 99% H_2/1% CO at 1 atm total pressure in a manner identical to that described for Figure 5. At time $t = 0$ s the flow was changed to 1000 cm^3 min^{-1} of 90% H_2/10% CO, with subsequent SER spectra acquired every 20 s. Typical results obtained by means of such a procedure are shown in Figure 6. Before the change in reactant ratio (bottom spectra), the 295 cm^{-1} ν_{Rh-O} band was clearly evident along with a trace of terminally adsorbed CO (480 cm^{-1}). However, the intensity of the 295 cm^{-1} feature was significantly diminished within 2 min after the reactant switch, with complete removal occurring by ca. 4−5 min. This result indicates that the removal of this oxygen species is facilitated by greater amounts of carbon monoxide.

Interestingly, the behavior of adsorbed CO was essentially unaffected over the range of H_2:CO ratios (99:1 to 80:20) examined here. As an example of this, typical SER spectra for a Rh surface heated in 100 cm^3 min^{-1} of 80% H_2/20% CO are presented in Figure 7. Of note is that the behavior of adsorbed

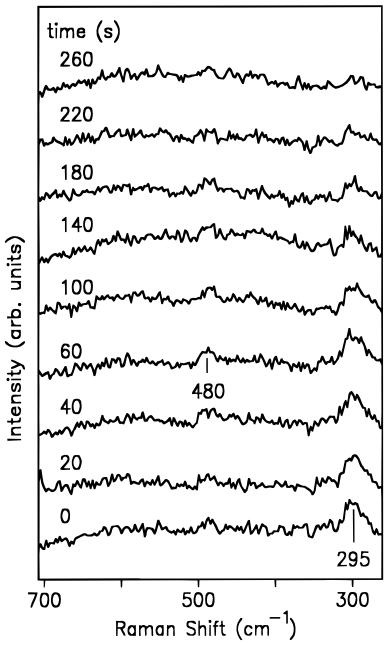

Figure 6. Real-time SER spectra of a Rh surface that was initially held at 300 °C in 1000 cm^3 min^{-1} of a 99% H_2/1% CO mixture at 1 atm. At $t = 0$ s the flow was switched to 1000 cm^3 min^{-1} of a 90% H_2/10% CO at 1 atm, with SER spectra recorded at 20 s intervals and a spectral acquisition time of 20 s.

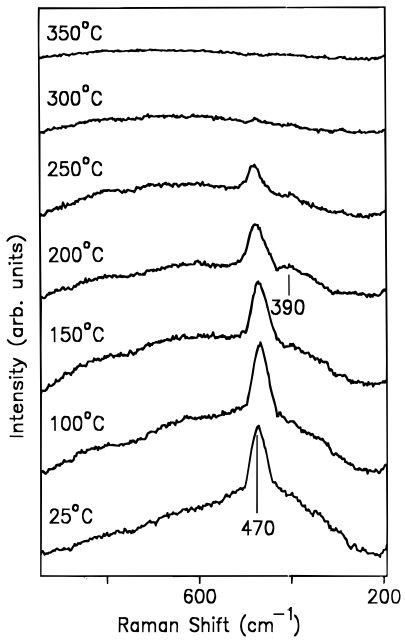

Figure 7. Temperature-dependent SER spectra of a Rh surface exposed to 100 cm^3 min^{-1} of a 80% H_2/20% CO mixture at 1 atm. The temperature was raised in a stepwise manner, starting at 25 °C, to the values indicated. Integration time for each spectrum was 10 s.

CO is identical to that observed in the former 99:1 H_2:CO case (Figure 5). Furthermore, the 295 cm^{-1} oxygen feature is not observed under these conditions, consistent with the results of the transient switching experiment (Figure 6).

In order to elucidate the possible influence of these adsorbed species upon the overall CO/H_2 reaction mechanism, complementary kinetic measurements were made by utilizing the small-volume reactor and higher-surface-area Rh thin-film samples described above (as well as actual polycrystalline Rh). Employing the same pretreatment procedure and reaction conditions as during the Raman experiments (Figures 5 and 7) allows direct correlations to be made between catalyst activity and surface

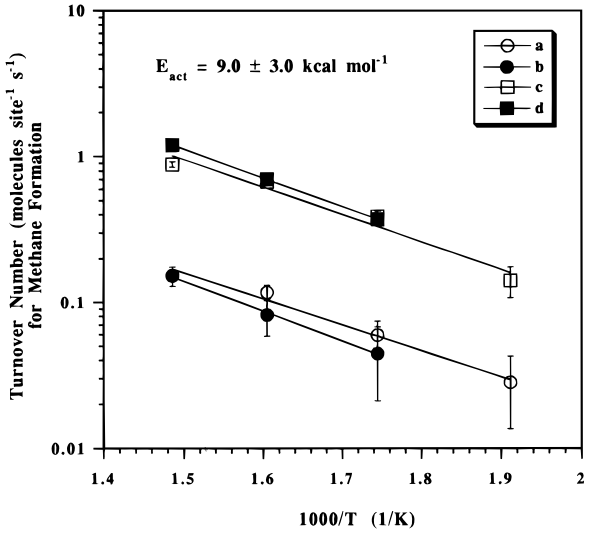

Figure 8. Line a: turnover numbers for methane formation using a Rh-coated gold wire pretreated at 150 °C in H_2 for 5 min and heated in 99% H_2/1% CO at 1 atm. Line b: same as (a) but with 80% H_2/20% CO at 1 atm. Line c: same as (a) but with 400 °C pretreatment. Line d: Same as (c) but using a polycrystalline Rh catalyst. The assumption was made that the site density was 10^{15} sites cm^{-2} for all rate calculations. The error bars represent the standard deviation of each point.

speciation. After reducing samples in H_2 at 150 or 400 °C for ca. 5 min, catalysts were subsequently exposed to either 99% H_2/1% CO or 80% H_2/20% CO reaction mixtures at 1 atm and heated in a stepwise periodic fashion identical to that utilized in Figures 5 and 7. Gas-phase compositions were measured utilizing a mass spectrometer (*vide supra*), and several *m*/*e* values were recorded to account for all possible products, which included CH_4 (16, 15), H_2O (18), CO_2 (44), CH_3OH (31, 32), CH_2O (30), C_2H_6 (28, 27), and C_3H_8 (44, 29). A series of kinetic results obtained using the above-mentioned pretreatment procedures and reaction conditions are presented in Figure 8. Assuming, as conventional, the presence of 10^{15} sites cm^{-2}, the reaction rates are presented as turnover numbers with units of molecules site^{-1} s^{-1}. Methane was the only detectable hydrocarbon product under all conditions studied. This is similar to the literature mentioned above for polycrystalline Rh,[1,2] where methane selectivity was typically 90−95%. While the high background level of water in the MS chamber made it impossible to monitor its formation, the absence of any other oxygen-containing species (e.g., CO_2, CH_3OH, CH_2O) suggests that H_2O was indeed being produced.

It is interesting to correlate the threshold temperature at which measurable reaction occurs for the catalysts pretreated at 150 °C in H_2 with the relative amount of CO on the surface, as deduced roughly from the ν_{Rh-C} band intensity. The amount of adsorbed CO decreases significantly from 250 to 300 °C for both reactant ratios (Figures 5 and 7), which coincides roughly with the first detectable levels of methane formation during the corresponding kinetic experiments (Figure 8, symbols a and b). Thus, it is plausible that the high coverage of CO is hindering methane formation at lower temperatures (<250 °C). This phenomenon has been observed during studies of CO hydrogenation on supported Rh catalysts,[4,6,8] with several explanations proffered. Koertz et al.[6] show that the activation energy for carbon monoxide dissociation is lowered as CO surface coverage decreases. This causes greater levels of CO dissociation at higher temperatures where the CO coverage begins to decrease, thus producing more of the active surface carbon that is presumably an intermediate for methane formation. Somewhat

related to this effect is the hypothesis that adsorbed CO blocks H_2 from adsorbing on active sites that are necessary for hydrogenation of the active carbon intermediate.[4] Therefore, the reaction rate increases when CO desorbs, and the coverage of hydrogen becomes significant. Comparison of the kinetic results for these two reactant ratios also suggests that the 295 cm^{-1} oxygen species (Figure 5) has little or no effect on the overall methanation rate. This is an indication that it is a "spectator" with regard to CO hydrogenation, perhaps residing at inactive surface sites. It is also interesting that the methanation rate is relatively unaffected by the change in reactant ratio (Figure 8, symbols a and b)

This high selectivity toward methane and the observed turnover numbers are partly consistent with one of the most comprehensive studies of CO hydrogenation on polycrystalline Rh.[1] However, the measured activation energy ($E_{act} = 9.0 \pm 3.0$ kcal mol^{-1}) is a factor of 2 smaller than that measured by Sexton and Somorjai.[1] To determine whether the low-temperature H_2 pretreatment of the surface (Figure 8, symbols a and b) might be causing this effect, several experiments were performed that involved pretreating both thin-film and bulk polycrystalline Rh surfaces at 400 °C in H_2 for 5 min. Figure 8 (symbols c and d) shows typical data obtained during reaction in 99% H_2/1% CO at 1 atm after this more rigorous pretreatment procedure was employed. While the turnover numbers are about 1 order of magnitude higher than those obtained with the 150 °C pretreatment, the activation energy remained essentially unchanged. However, methane formation could not be detected upon subsequent reaction at lower temperatures over these catalysts unless the surface was rigorously pretreated again in pure H_2, indicating that surface deactivation was occurring. Therefore, a more plausible explanation for the low activation energy noted above may be that the surface becomes progressively deactivated through site blocking by contaminants as the sample is heated to higher temperatures, partly nullifying the temperature-induced rate increases as prescribed by the Arrhenius law. While Sexton and Somorjai observed no catalyst deactivation during their experiments under similar pressures,[1] this is probably a result of the much more rigorous pretreatment cleaning procedure (including annealing at 1000 °C and ion bombardment in ultrahigh vacuum) than we had available in the present study.

CO Adsorption/Desorption Mechanism. A less-studied aspect of CO adsorption and reaction with hydrogen on Rh is the rate and mechanism by which gas-phase CO exchanges with adsorbed CO on the catalyst surface. While CO desorption from rhodium surfaces *into vacuum* has been well characterized for polycrystalline Rh,[1,18] it has long been known that the adsorption/desorption kinetics are significantly enhanced by the presence of gas-phase CO. Yates et al.[44,45] observed that adsorbed ^{13}CO was completely replaced in 11 min by ^{12}CO at 22 °C when a surface saturated with the former was exposed to 50 Torr of the latter. In order to explain the facilitation of this exchange at temperatures well below those reported for thermal desorption (150−200 °C),[1,18] it was postulated that the high pressure of CO produced a transient surface intermediate (e.g., $Rh-(CO)_x$) that was responsible for this behavior. More recently, Zhai and co-workers have reported extensive investigations of this assisted desorption process on Rh(111) in the presence of low CO pressures.[46−48] The most recent of these investigations was performed in the presence of $(2-9) \times 10^{-8}$ Torr of CO.[46] The apparent activation energy for the exchange of CO on the surface was about 8.5 kcal mol^{-1}, significantly lower than the activation energies of 30−32 kcal mol^{-1} reported for desorption into vacuum from various Rh surfaces.[1,18,46] Thus, the authors postulated some other mechanism must be responsible for the CO exchange at lower temperatures. Lombardo and Bell[49] have succeeded in modeling CO exchange phenomena measured for polycrystalline Pd[50,51] and Ni(100)[52] using Monte Carlo simulations and propose that the observed behavior results from the effects that the repulsive lateral interactions have on the activation energy for desorption.

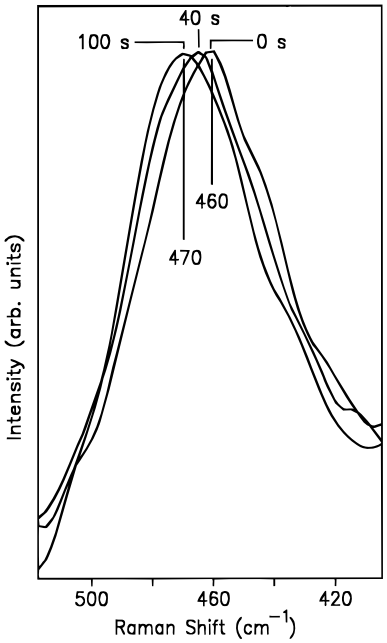

Figure 9. Real-time SER spectra of a Rh surface at 200 °C during $^{13}CO/^{12}CO$ isotope switching in an 80% H_2/20% CO mixture at 1 atm. After holding the sample in a mixture containing ^{13}CO, 1400 cm^3 min^{-1} of the mixture containing ^{12}CO was flowed through though the reactor at $t = 0$ s. Spectra were recorded at 10 s intervals with an acquisition time of 10 s. The spectra were smoothed using the Savitsky−Golay approach, and only selected spectra are shown here.

While a few recent studies of the $CO-H_2$ reaction have directly measured the rate at which CO adsorbs/desorbs on the catalyst surface at higher pressures,[3,53] there has been no systematic effort made to elucidate the mechanism by which this exchange occurs. One obstacle to monitoring this process at elevated pressures has been the challenge of acquiring high-quality vibrational spectra with a rapidity sufficient to follow the switching in real time. Thus, the ability to record SER spectra on a seconds time scale provides a novel method of probing this process directly. As this study was conducted at pressures which were 9−10 orders of magnitude higher than those used by Song et al.,[46] several differences were expected to be found between the observed kinetics, most notably in the pressure dependencies. Also of particular interest was discerning the effect (if any) that hydrogen has on this process.

Transient $^{13}CO/^{12}CO$ Exchange Experiments. Transient response experiments involved switching from a flow containing ^{13}CO to one with ^{12}CO at a total pressure of 1 atm and monitoring the time-dependent spectral response. As an illustration of this protocol, typical SER spectra for such an isotopic substitution in the presence of H_2 are presented in Figure 9. The spectra for increasing times are presented right to left, with only selected spectra presented for clarity. In this case, the spectra have also been smoothed using the Savitsky−Golay approach. A reduced sample was exposed to a 20% ^{13}CO/80% H_2 mixture at 1 atm of total pressure and 25 °C. After heating to 200 °C and allowing the spectra to become time-independent, 1400 cm^3 min^{-1} of 20% ^{12}CO/80% H_2 at 1 atm was flowed through the reactor, with SER spectra being acquired every 10

s. This high flow rate was sufficient to essentially completely flush out the reactor of the previous mixture within 10 s (i.e., 3 residence times). Before the switch, the 10 cm^{-1} downshifted ν_{Rh-C} band of terminal ^{13}CO is evident at 460 cm^{-1}. It is evident upon careful examination that the adsorbed ^{13}CO is replaced by ^{12}CO within ca. 100 s, with the 460 cm^{-1} feature shifting upward in frequency to a final value of 470 cm^{-1}.

Essentially identical transient response experiments were performed under three different sets of conditions (100% CO, 20% CO/80% H_2, and 1% CO/99% H_2) at 1 atm total pressure and varying temperature. The results indicate that, at least up to 200 °C, the presence of H_2 has no significant effect on the CO exchange rates. Furthermore, varying the partial pressure of ^{12}CO by 2 orders of magnitude, 8−760 Torr, produced no detectable change in the CO turnover rate, indicating a zero-order dependence on CO partial pressure in this range.

The observed lack of dependence on gas-phase CO concentration at our elevated pressures contrasts the results of Zhai and co-workers,[46−48] who have observed a first-order dependence on CO partial pressure below 10^{-5} Torr. While Yates et al.[44,45] and Song et al.[46] suggest that the CO exchange proceeds through some intermediate species (possibly a gem dicarbonyl), this explanation cannot adequately explain the zero-order dependence of the exchange on gas-phase CO concentration at higher pressures. The experiments in the literature (and here) have been performed under conditions where almost all possible chemisorption sites at a given temperature and CO partial pressure are occupied. However, surface sites that are energetically less favorable, yet feasible, for CO chemisorption should still be available under these conditions. Specifically, these sites may facilitate the formation of metastable Rh−CO intermediates capable of exchanging with other adsorbed CO molecules. One can propose a mechanistic scheme for this process along the following lines,

$$^{12}CO_{(g)} + [*] \leftrightarrow {}^{12}CO{-}[*] \quad (3a)$$

$$^{12}CO{-}[*] + {}^{13}CO_{(ads)} \leftrightarrow {}^{12}CO_{(ads)} + {}^{13}CO{-}[*] \quad (3b)$$

$$^{13}CO{-}[*] \leftrightarrow {}^{13}CO_{(g)} + [*] \quad (3c)$$

where $[*]$ denotes an energetically unfavorable site. Assuming that the surface concentration of $^{13}CO{-}[*]$ is negligible (which would be expected due to the absence of gaseous ^{13}CO during the switch) and using the pseudo-steady-state approximation on $^{12}CO{-}[*]$, a rate equation with the following form is derived

$$\frac{d\theta_{13}}{dt} = -k_e\theta_{13}\left[\frac{KP_{12}}{1+KP_{12}}\right] \quad (4)$$

where θ_{13} is the ^{13}CO coverage, k_e is the rate constant for the exchange between $^{12}CO{-}[*]$ and ^{13}CO (eq 3b, forward), K is the equilibrium constant from eq 3a, and P_{12} is the partial pressure of ^{12}CO. This mechanism and accompanying rate equation are well-known in heterogeneous catalysis[54] and are closely analogous to the well-known Michaelis−Menten kinetics for enzymatic systems.[55] As the pressure increases, the $[*]$ sites are filled until saturation is reached, at which point the exchange process undergoes a transition from a first-order dependence on CO partial pressure[46−48] to a pressure-independent behavior, the rate now being controlled solely by the kinetics of the exchange reaction. Thus, for the present high-pressure conditions,

$$d\theta_{13}/dt = -k_e\theta_{13} \quad (5)$$

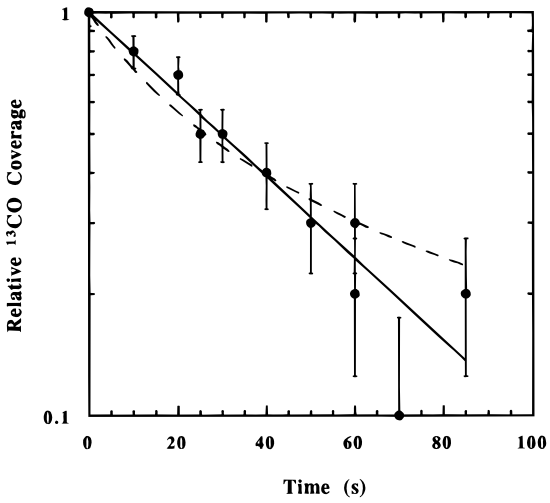

Figure 10. Relative ^{13}CO coverage as a function of time during $^{13}CO/^{12}CO$ switching for the conditions described in Figure 9. Data points presented here include those from the experiment described by Figure 9. Least-square fits to first- and second-order kinetic models are represented by the solid and dashed lines, respectively. The error bars represent the standard deviation of each point.

The predicted θ_{13} reaction order may be verified and the rate constant for the exchange process (k_e) estimated by analysis of the $^{13}CO/^{12}CO$ exchange results (*vide supra*). Assuming that there is no dipole−dipole coupling and that large overlap exists between the $\nu_{Rh-^{13}C}$ and $\nu_{Rh-^{12}C}$ bands, the observed ν_{Rh-C} frequency will essentially vary linearly with ^{13}CO coverage. Using these assumptions, a plot showing the decrease in fractional ^{13}CO coverage ($\theta_{13}/\theta_{13,o}$) as a function of time may be produced for each set of transient experiments. This is achieved by carefully measuring the change in the band frequency as a function of time and normalizing to the overall shift, 10 cm^{-1}. An example of such an analysis applied to data from isotope exchange conducted at 20% CO/80% H_2 and 200 °C is presented in Figure 10. Note that the data points utilized here include those obtained during the experiment presented in Figure 9. Performing linear regression on the data with a kinetic model that was first order in θ_{13} produced notably better fits than for higher-order cases. (A second-order fit is shown in Figure 10 for comparison.) Similarly, the exchange process was most effectively modeled by first-order kinetics under all other conditions studied (*vide supra*), consistent with the derived rate law above (5). We note again that the presence of H_2 in the gas phase had no observable effect on the exchange process under these conditions.

In order to gain insight into the mechanism for CO turnover under reaction conditions, an Arrhenius plot was constructed (Figure 11) consisting of the first-order rate constants obtained at different temperatures under 20% CO/80% H_2 at 1 atm. It is immediately evident that the rate at which CO is exchanging ($k_{d,tot}$) is only weakly activated ($E_{d,tot} = 1 \pm 0.1$ kcal mol^{-1}) at temperatures from 25 to 100 °C, with a small preexponential factor ($k_{do,tot} = 0.035 \pm 0.003$ s^{-1}). As no thermal desorption is expected to occur by these temperatures, $E_{d,tot}$ and $k_{do,tot}$ are essentially equal to E_e and k_{eo}, respectively. This activation energy is much lower than the ca. 8.5 kcal mol^{-1} observed at lower pressures (10^{-8} Torr) by Song et al.,[46] again suggesting a change in the exchange mechanism with increasing CO pressure (*vide supra*). The observed 5-fold increase in the activation energy between 150 and 200 °C marks the emergence of competing pathways for CO removal, including thermal desorption and/or reaction with hydrogen. For instance, based on reported TPD spectra of CO from polycrystalline Rh,[1,18] both

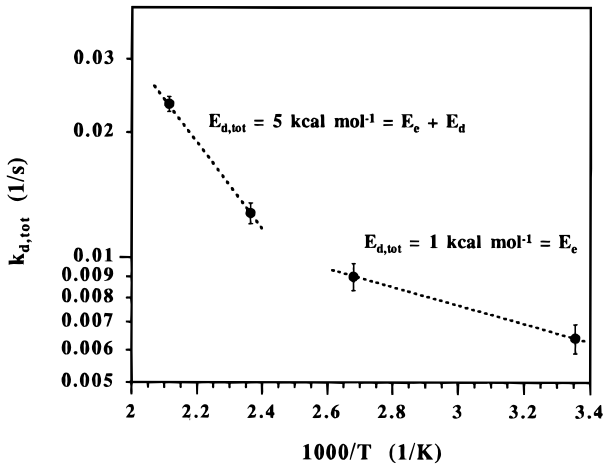

Figure 11. Arrhenius plot consisting of overall desorption first-order rate constants ($k_{d,tot}$) obtained during $^{13}CO/^{12}CO$ isotope switching at various temperatures in 80% H_2/20% CO at 1 atm.

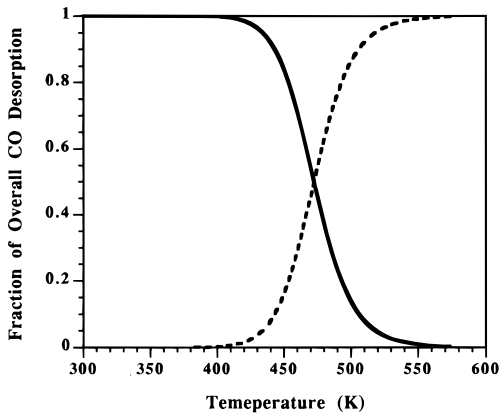

Figure 12. Calculated fractions of overall CO desorption accounted for by the exchange (solid line) and thermal (dashed line) pathways as a function of temperature. These data were produced by using the kinetic parameters and generating a series of points over the wide temperature range indicated.

CO exchange (3b) *and* thermal desorption/adsorption would be taking place to a significant extent at temperatures greater than 150 °C. Thus, the overall exchange first-order rate constant ($k_{d,tot}$) measured at these (and actually all) temperatures can be represented as a sum of the rate constants for each of the competing first-order processes:

$$k_{d,tot} = k_e + k_d = k_{eo} \exp\left(\frac{-E_e}{RT}\right) + k_{do} \exp\left(\frac{-E_d}{RT}\right) \quad (6)$$

where k_e and k_d are first-order rate constants, k_{eo} and k_{do} are preexponential factors, E_e and E_d are activation energies, R is the gas constant, and T is temperature. The subscript e refers to the exchange reaction while d refers to thermal desorption. By employing the kinetic parameters obtained for the exchange reaction at 25 and 100 °C (k_e), assuming that $k_{do} = 10^{13}$ s^{-1},[17] and using the $k_{d,tot}$ values obtained for 150 and 200 °C (Figure 10), the activation energy for thermal desorption under these high-pressure conditions was estimated. A value of $E_d = 31.3 \pm 3$ kcal mol^{-1} is obtained, which is consistent with previously reported values for CO desorption from polycrystalline Rh.[1,18]

Using these kinetic parameters, both the exchange and thermal desorption rate constants may be calculated for a wide range of temperatures. From these a plot was constructed that illustrates the relative importance of exchange and thermal desorption to the overall CO turnover rate as a function of temperature (Figure 12). As can be seen, the assisted pathway is dominant for temperatures up to 150 °C. However, at higher temperatures the rate of the thermal process eclipses that of the assisted route, accounting for almost all of the CO desorption by 250 °C. Perhaps not surprisingly, thermal desorption begins to dominate at the temperature for which maxima in TPD curves have been observed during CO adsorption on polycrystalline Rh.[1,18] This observed change in the dominant CO desorption pathway underscores the major differences that can exist between adsorption/desorption processes in higher-pressure and ultrahigh-vacuum environments.

Having examined the kinetics for assisted CO desorption at elevated pressures, it is interesting to analyze the lower pressure regime investigated by Song et al. on Rh(111).[46] Utilizing their pressure-dependent ($(2-9) \times 10^{-8}$ Torr) CO coverage versus time data[46] with the kinetic parameters for k_e ($k_{eo} = 0.035 \pm 0.003$ s^{-1}, $E_e = 1 \pm 0.1$ kcal mol^{-1}) in eq 4, the equilibrium constant, K, may be calculated. Using the reported apparent activation energy of 8.5 ± 0.5 kcal mol^{-1}, both the preexponential factor ($K_o = (3.0 \pm 0.4) \times 10^{11}$ Torr^{-1}) and a free energy of activation ($\Delta G_{act} = 7.5 \pm 0.6$ kcal mol^{-1}) were obtained. By varying the pressure from 1×10^{-8} to 760 Torr and examining the magnitude of P_{12} in eq 4, it was determined that the exchange is an equilibrium-controlled process with a first-order pressure dependence below ca. 10^{-4} Torr. In contrast, higher than ca. 10^{-2} Torr the process exhibits no pressure dependence and is solely controlled by kinetics of the exchange mechanism (3b).

Concluding Remarks

In this paper we have presented *in-situ* monitoring of several processes occurring on a polycrystalline rhodium catalyst in the presence of ambient pressures of CO and H_2. This has been accomplished through the use of surface-enhanced Raman spectroscopy (SERS) and mass spectrometry (MS). Several pieces of insight have been gained:

1. The dominant desorption pathway for adsorbed CO from Rh in the presence of high CO partial pressures appears to change from a weakly activated first-order exchange process at lower temperatures (≤150 °C) to first-order thermal desorption at higher temperatures (≥200 °C). The exchange process likely proceeds via adsorption of CO molecules on unstable, energetically unfavorable sites, followed by exchange with chemisorbed CO. Interestingly, the presence of hydrogen had no noticeable effect on the exchange rates. The exchange mechanism itself also falls into two regimes, one of which is dependent on pressure ($<10^{-4}$ Torr) and another that is controlled by the exchange kinetics ($>10^{-2}$ Torr).

2. Methane was observed to be the major product, with kinetic measurements indicating that the removal of CO from the surface between 250 and 300 °C causes the reaction rate to increase dramatically, possibly by freeing active sites for hydrogen adsorption. Catalyst deactivation was observed after methanation at 400 °C under all reaction conditions, most likely as a result of impurities in the reaction system and the lack of rigorous oxidation/reduction pretreatments of the catalyst at high temperatures.

3. While only CO was observed on the catalyst surface when utilizing reactive mixtures with greater than 1% CO, a form of adsorbed oxygen was also present at higher temperatures when smaller amounts of CO were reacted. As the presence of this adsorbed oxygen did not affect overall rates for or selectivity toward CH_4 production, it is probable that this species resides at sites not involved in the CO hydrogenation reaction.

4. Some CO dissociation was detected at temperatures as low as 100 °C on these polycrystalline surfaces, as discerned

by the temperature-dependent behavior of the 470 cm^{-1} ν_{Rh-C} feature. The apparent concurrent formation of surface carbonate may also result from this dissociation process. Moreover, the presence of gas-phase CO or H_2 appears to hamper CO dissociation at lower temperatures, most likely due to blocking of the sites necessary for the process to proceed.

5. The presence of hydrogen causes some adsorbed CO to switch from a terminal configuration ($\nu_{Rh-C} = 470$ cm^{-1}) to 2-fold bridging sites ($\nu_{Rh-C} = 390$ cm^{-1}) at elevated temperatures (ca. 200 °C), possibly as a result of repulsive forces within the adlayer.

Acknowledgment. This work was supported by a grant to C.G.T. and M.J.W. (CTS-9312008) from the National Science Foundation.

References and Notes

(1) Sexton, B. A.; Somorjai, G. A. *J. Catal.* **1977**, *46*, 167.
(2) Castner, D. G.; Blackadar, R. L.; Somorjai, G. A. *J. Catal.* **1980**, *66*, 257.
(3) Balakos, M. W.; Chuang, S. S. C.; Srinivas, G.; Brundage, M. A. *J. Catal.* **1995**, *157*, 51.
(4) Zhang, Z.; Kladi, A.; Verykios, X. E. *J. Catal.* **1995**, *156*, 37.
(5) Efstathiou, A. M.; Chafik, T.; Bianchi, D.; Bennet, C. O. *J. Catal.* **1994**, *148*, 224.
(6) Koertz, T.; Welters, W. J. J.; van Santen, R. A. *J. Catal.* **1992**, *134*, 1.
(7) (a) Iizuka, T.; Tanaka, Y.; Tanabe, K. *J. Catal.* **1982**, *76*, 1. (b)-Fisher, I. A.; Bell, A. T. *J. Catal.* **1996**, *162*, 54.
(8) Solymosi, F.; Tombacz, I.; Kocsis, M. *J. Catal.* **1982**, *75*, 78.
(9) Guglielminotti, E.; Giamello, E.; Pinna, F.; Strukul, G.; Martinengo, S.; Zanderighi, L. *J. Catal.* **1994**, *146*, 422.
(10) Chudeck, J. A.; McQuire, M. W.; McQuire, G. W.; Rochester, C. H. *J. Chem. Soc., Faraday Trans.* **1994**, *90*, 3699.
(11) McQuire, M. W.; Rochester, C. H.; Anderson, J. A. *J. Chem. Soc., Faraday Trans.* **1991**, *87*, 1921.
(12) Watson, P. R.; Somorjai, G. A. *J. Catal.* **1981**, *72*, 347.
(13) Solymosi, F.; Erdohelyi, A. *Surf. Sci.* **1981**, *110*, L360.
(14) Kroeker, R. M.; Kaska, W. C.; Hansma, P. K. *J. Catal.* **1980**, *61*, 87.
(15) Worley, S. D.; Mattson, G. A.; Caudill, R. *J. Phys. Chem.* **1983**, *87*, 1671.
(16) McKee, M. L.; Dai, C. H.; Worley, S. D. *J. Phys. Chem.* **1988**, *92*, 1056.
(17) Chudeck, J. A.; McQuire, M. W.; Rochester, C. H. *J. Catal.* **1992**, *135*, 358.
(18) Gorodetskii, V. V.; Nieuwenhuys, B. E. *Surf. Sci.* **1981**, *105*, 299.
(19) Yates, J. T., Jr.; Williams, E. D.; Weinberg, W. H. *Surf. Sci.* **1980**, *91*, 562.
(20) Castner, D. G.; Somorjai, G. A. *Surf. Sci.* **1979**, *83*, 60.
(21) Ren, D.-M.; Liu, W. *Surf. Sci.* **1990**, *232*, 316.
(22) Liu, W.; Ren, D.-M. *Surf. Sci.* **1990**, *232*, 323.
(23) Cho, B. K.; Stock, C. J. *J. Catal.* **1989**, *117*, 202.
(24) Wilke, T.; Gao, X; Takoudis, C. G.; Weaver, M. J. *Langmuir* **1991**, *7*, 714.
(25) Wilke, T.; Gao, X; Takoudis, C. G.; Weaver, M. J. *J. Catal.* **1991**, *130*, 62.
(26) Tolia, A., Wilke, T., Weaver, M. J.; Takoudis, C. G. *Chem. Eng. Sci.* **1992**, *47*, 2781.
(27) Tolia, A. A.; Weaver, M. J.; Takoudis, C. G. *J. Vac. Sci. Technol. A* **1992**, *11 (4)*, 2013.
(28) Tolia, A. A.; Smiley, R. J.; Delgass, W. N.; Takoudis, C. G.; Weaver, M. J. *J. Cat.* **1994**, *150*, 56.
(29) Tolia, A. A.; Williams, C. T.; Takoudis, C. G.; Weaver, M. J. *J. Phys. Chem.* **1995**, *99*, 4599.
(30) Tolia, A. A.; Williams, C. T.; Weaver, M. J.; Takoudis, C. G. *Langmuir* **1995**, *11*, 3438.
(31) Williams, C. T.; Tolia, A. A.; Weaver, M. J.; Takoudis, C. G. *Chem. Eng. Sci.* **1996**, *51*, 1673.
(32) Williams, C. T.; Tolia, A. A.; Chan, H.; Takoudis, C. G.; Weaver, M. J. *J. Catal.* **1996**, *163*, 63.
(33) Gao, P.; Gosztola, D.; Leung, L.-W. H.; Weaver, M. J. *J. Electroanal. Chem.* **1987**, *233*, 211.
(34) Leung, L.-W. H.; Weaver, M. J. *J. Am. Chem. Soc.* **1987**, *109*, 5113.
(35) Leung, L.-W. H.; Weaver, M. J. *Langmuir* **1988**, *4*, 1076.
(36) a) Kai, S.; Chaozhi, W.; Guangzhi, X. *Spectrochim. Acta* **1989**, *45A*, 1029. (b) Sasaki, Y.; Iwasaki, N.; Nishina; Y. *Surf. Sci.* **1988**, *198*, 541. (c) Stuve, E. M.; Madix, R. J.; Sexton, B. A. *Chem. Phys. Lett.* **1982**, *89*, 48.
(37) Sachtler, W. M. H.; Ichikawa, M. *J. Phys. Chem.* **1986**, *90*, 4752.
(38) de Koster, A.; Jansen, A. P. J.; Geerlings, J. J. C.; van Santen, R. A. *Faraday Discuss. Chem. Soc.* **1989**, *87*, 262.
(39) Richter, L. J.; Gurney, B. A.; Ho, W. *J. Chem. Phys.* **1987**, *86*, 477.
(40) Richter, L. J.; Germer, T. A.; Ho, W. *Surf. Sci.* **1988**, *195*, L182.
(41) Desilvestro, J.; Weaver, M. J. *J. Electroanal. Chem.* **1986**, *209*, 377.
(42) Campbell, C. T.; White, J. M. *J. Catal.* **1978**, *54*, 289.
(43) Thiel, P. A.; Yates, J. A.; Weinberg, W. H. *Surf. Sci.* **1979**, *82*, 22.
(44) Yates, J. T., Jr.; Duncan, T. M.; Worley, S. D.; Vaughan, R. W. *J. Chem. Phys.* **1979**, *70*, 1219.
(45) Yates, J. T., Jr.; Duncan, T. M.; Vaughan, R. W. *J. Chem. Phys.* **1979**, *71*, 3908.
(46) Song, Z.; Lu, R.; Lou, N.; Zhai, R. *Chem. Phys. Lett.* **1994**, *217*, 142.
(47) Guo, X.; Song, Z.; Ziang, L.; Xiang, N.; Zhai, R. *Catal. Lett.* **1992**, *12*, 7.
(48) Guo, X.; Xin, M.; Zhai, R. *J. Phys. Chem.* **1994**, *98*, 7145.
(49) Lombardo, S. J.; Bell, A. T. *Surf. Sci.* **1991**, *245*, 213.
(50) Yamada, T.; Onishi, T.; Tamaru, K. *Surf. Sci.* **1983**, *133*, 533.
(51) Yamada, T.; Onishi, T.; Tamaru, K. *Surf. Sci.* **1985**, *157*, L389.
(52) Yates, J. T., Jr.; Goodman, D. W. *J. Chem. Phys.* **1980**, *73*, 5371.
(53) Efstathiou, A. M.; Chafik, T.; Bianchi, D.; Bennet, C. O. *J. Catal.* **1994**, *147*, 24.
(54) For example see: Boudart, M.; Djega-Mariadassou, G. *Kinetics of Heterogeneous Catalytic Reactions*, Princeton University Press: Princeton, NJ, 1984, p 92.
(55) For example see: Moore, J. W.; Pearson, R. G. *Kinetics and Mechanism*; Wiley: New York, 1981; p 379.